



## Changes to Charge and Defects in Dielectrics from Ion and Photon Fluences during Plasma Exposure

H. Ren,<sup>a</sup> Y. Nishi,<sup>b</sup> and J. L. Shohet<sup>a,z</sup>

<sup>a</sup>Plasma Processing and Technology Laboratory and Department of Electrical and Computer Engineering, University of Wisconsin-Madison, Madison, Wisconsin 53706, USA

<sup>b</sup>Stanford University, Stanford, California 94305, USA

A methodology is introduced to investigate the effects of ion and photon fluences on dielectrics during plasma exposure. Ion and photon fluences were separated using a capillary-array window. The fluences can be varied separately by varying the plasma parameters. Most of the charge accumulation came from the ion fluence, while the photon fluence introduced most of the defect-state modifications. It was further shown that during plasma exposure, UV photons can penetrate through the dielectric layer and cause modifications of the defect states. Based on the results, optimized conditions were found to minimize both the charge accumulation and the defect-state formation during plasma exposure.

© 2010 The Electrochemical Society. [DOI: 10.1149/1.3524403] All rights reserved.

Manuscript submitted October 5, 2010; revised manuscript received November 15, 2010. Published December 7, 2010.

Plasma-processing-induced damage has been an important issue in manufacturing microelectronic devices.<sup>1</sup> Damage includes dielectric charging,<sup>2</sup> defect-state formation,<sup>3,4</sup> chemical and physical changes,<sup>5,6</sup> and mechanical degradation.<sup>7</sup> This processing-induced damage can be from ions, photons, and radicals striking the dielectric.<sup>8,9</sup> Among these damage sources, ion bombardment has been believed to be the greatest for changing the properties of dielectrics.<sup>8</sup> However, such ion-induced damage may only happen within an ion penetration depth.<sup>10</sup> Vacuum ultraviolet (VUV)-modified dielectric layers were typically shown to be deeper than the ion-modified layer.<sup>11</sup>

Based on this, it is our contention that, within the dielectric, beyond the ion penetration depth, photons are responsible for the damage in this region, while on the surface, the damage is primarily caused by ions. Here, the two sources of damage generated during plasma processing will be considered to determine the effects of ion and photon fluences on the damage. They are charge accumulation and defect-state formation. This article establishes the roles of photons and ions in charge accumulation and defect-state formation in dielectric materials.

In order to determine this, electron-spin resonance (ESR) spectroscopy measurements were made to detect the modifications of the interfacial defect states and surface potential measurements with a Kelvin probe were used to detect the charge accumulation. Previously, VUV and UV exposures from synchrotron radiation and HgAr lamp have been shown to be responsible for the interlayer defect-state modifications in the dielectrics.<sup>12</sup>

As a test sample, we used atomic-layer-deposited 20-nm-thick HfO<sub>2</sub> on (100)Si. Note that the dielectric sample is ultrathin which guarantees a modification of the interfacial defects. The resistivity of silicon substrate is 4000 Ω cm which is needed to obtain effective ESR measurements.<sup>13</sup> An electron cyclotron resonance plasma system<sup>9</sup> was utilized to provide the plasma exposure of the dielectric films. Argon plasma was used to minimize the creation of free radicals,<sup>14</sup> so that the ion and photon bombardments were the primary sources of potential damage.

To vary the ion and photon fluences, pressure and microwave power were scanned between ranges of 5 and 30 mTorr and 100 and 400 W, respectively. The pressure was varied using a mass-flow controller. For any combination of pressure and power, the ion flux can be calculated using the continuity equation<sup>15</sup> as

$$\Gamma_i = n_i v_i = n_{is} \chi u_B \quad [1]$$

where  $\Gamma_i$  is the ion flux incident on the dielectric sample and  $n_i$  and  $v_i$  are the ion density and velocity in the vicinity of the dielectric sample, respectively. Based on this, the ion flux incident on the

sample should be equal to the flux at the edge of the sheath, where  $n_{is}$  is the ion density in the bulk plasma,  $\chi$  is the density-drop coefficient in the presheath,<sup>16,17</sup> and  $u_B$  is the Bohm velocity for the sheath formation.<sup>18</sup> The ion density is set equal to the electron density and the Bohm velocity can be expressed as

$$n_{is} = n_e ; \quad u_B = \sqrt{\frac{eT_e}{M}} \quad [2]$$

where  $n_e$  and  $T_e$  represent the electron density and the electron temperature which were measured with a Langmuir probe.<sup>19</sup>  $M$  is the ion mass. To maintain continuity, the ion flux at the edge of the presheath should be equal to the flux at the edge of the sheath, as expressed in the following equation

$$n_{is} \chi u_B = n_{is} v_i \quad \text{as } v_i = \sqrt{\frac{eT_i}{M}} \quad [3]$$

where  $v_i$  is the ion thermal velocity and  $T_i$  is the ion temperature. In this experiment, the plasma is highly nonthermal, so that the ion temperature can be approximated to be room temperature. Thus, the density-drop coefficient in the presheath can be expressed as

$$\chi \approx \sqrt{\frac{T_i}{T_e}} \quad [4]$$

Using Eq. 1 and 4, the ion flux can be obtained.

The photon flux was measured with a vacuum-ultraviolet monochromator. With the monochromator, we can measure the time-integrated photon flux over a range of wavelengths from 50 to 300 nm. Both the in situ ion flux and photon fluxes are shown in Fig. 1. From Fig. 1, it can be seen that within the ranges of the plasma pressure and power used here, an increase in both pressure and power will lead to a higher ion flux. On the other hand, in order to get a higher photon flux, either a lower pressure or a higher power is needed.

With each combination of pressure and power, plasma exposure was made for 10 min. Time integrated, in situ measurements of ion flux and photon flux yield their respective fluences. After plasma exposure, the surface potential and defect-state concentrations were measured with a Kelvin probe and ESR spectroscopy, respectively.

Figure 2 shows the surface potential of the dielectric after plasma exposure as a function of ion and photon fluences. The surface potential for each combination of plasma pressure and power was computed as an average value over the dielectric surface that was exposed to the plasma. This allows us to convert the plasma conditions (pressure and power) directly into ion and photon fluences.

Contours of constant surface potential are also shown in Fig. 2. It can be seen that as the ion fluence increases, the average surface potential after exposure tends to increase correspondingly. However, an increase in the photon fluence does not lead to a significant

<sup>z</sup> E-mail: shohet@engr.wisc.edu

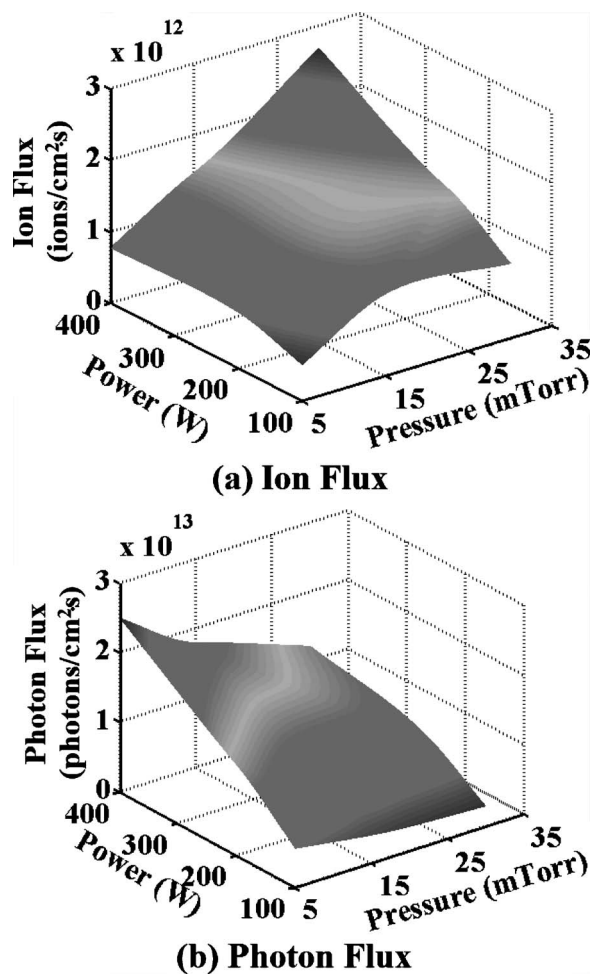


Figure 1. (a) Ion flux and (b) photon flux as functions of microwave power and pressure.

change of the surface potential. This indicates that the ion fluence dominates charge accumulation during plasma exposure. In addition, with the consideration of results from Ref. 9, we conclude that ion bombardment is critical in determining the charge accumulation on the dielectric due to ion sticking at the dielectric surface, while photon bombardment also contributes to the trapped-charge accumulation within the dielectric layer.

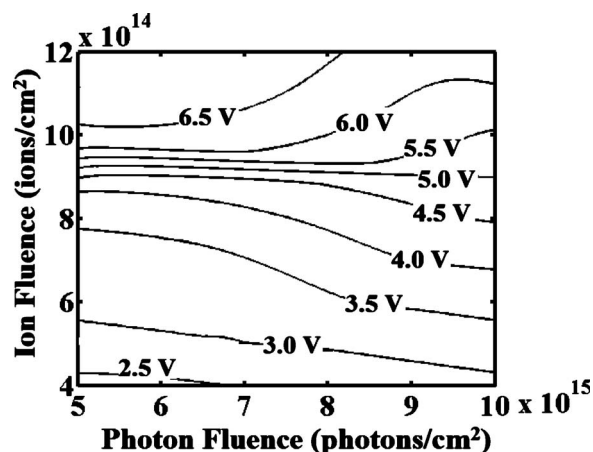


Figure 2. Surface potential as a function of ion and photon fluences.

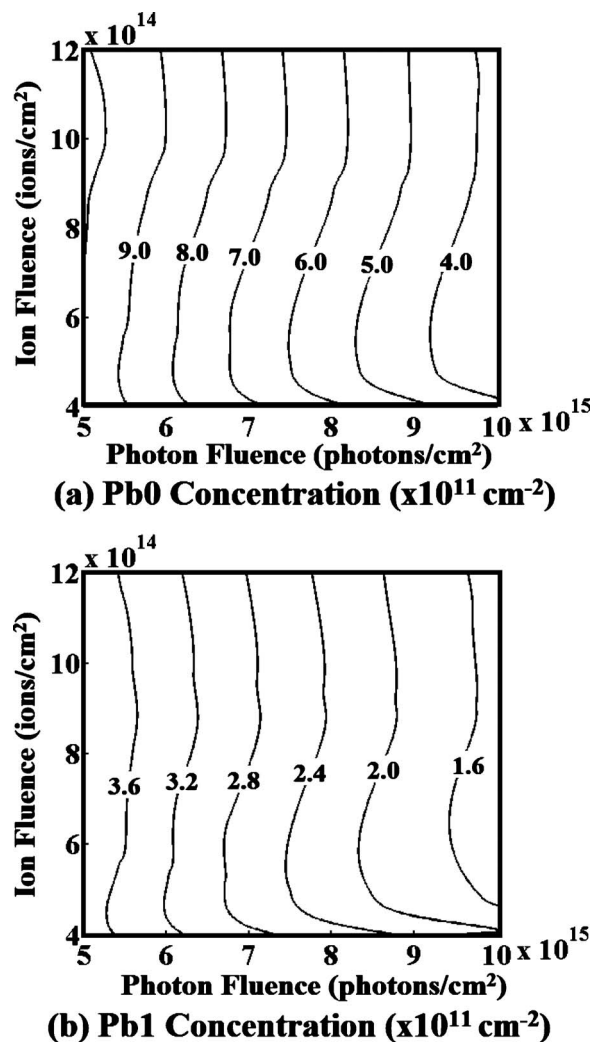
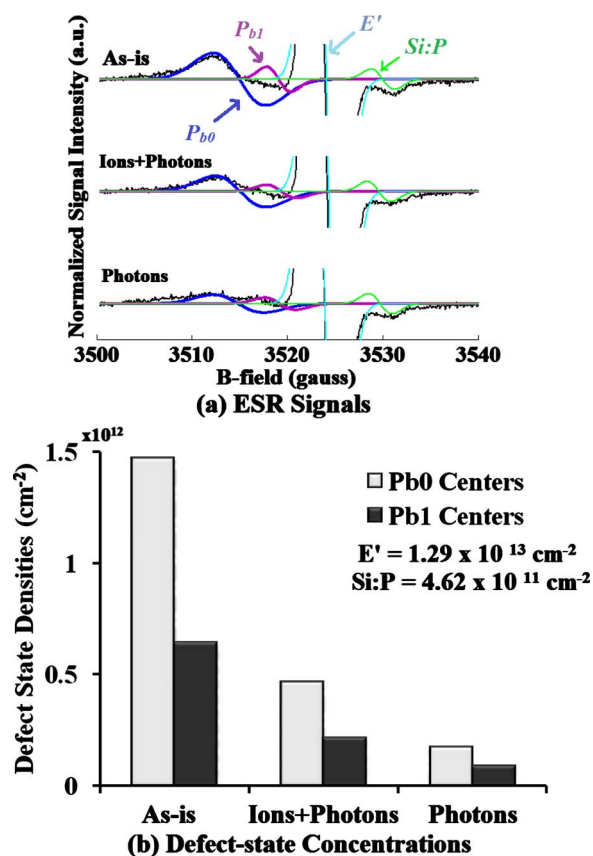


Figure 3. (a)  $P_{b0}$  and (b)  $P_{b1}$  concentrations as functions of ion and photon fluences. The as-deposited  $\text{HfO}_2$  has concentrations of  $1.16 \times 10^{12}$  and  $4.28 \times 10^{11} \text{ cm}^{-2}$  for  $P_{b0}$  and  $P_{b1}$  centers, respectively.

We utilize ESR spectroscopy to examine the modification of silicon dangling defects ( $P_b$ -type centers) after plasma exposure. Figure 3 shows the results. Because the silicon substrate has (100) orientation, silicon dangling bonds at the interlayer including both  $P_{b0}$  and  $P_{b1}$  centers were expected to increase in concentration.<sup>20</sup> Unexposed  $\text{HfO}_2$  has defect concentrations of  $1.16 \times 10^{12}$  and  $4.28 \times 10^{11} \text{ cm}^{-2}$  for  $P_{b0}$  and  $P_{b1}$  centers, respectively.

From Fig. 3, it is seen that the  $P_b$  concentration depends mainly on the photon fluence. As the photon fluence increases, the  $P_b$  concentration decreases. From previous work,<sup>12</sup> it was shown that  $P_b$  centers can be depleted by UV exposure. This implies that most of the UV photons from plasma exposure can penetrate through the 20-nm dielectric layer and reduce the  $P_b$  concentrations, while ions can barely penetrate into the interlayer and modify the defect states. A photon fluence of  $1 \times 10^{16}$  photons/ $\text{cm}^2$  can reduce most of the dangling defects.

Thus, we have found that ion bombardment influences dielectric films primarily at the surface, as evidenced by the surface charge accumulation. On the other hand, photon bombardment modifies the interlayer defect states as evidenced by changes in the defect densities. Importantly, we have found that 7.2 eV VUV exposure increases the  $P_b$  concentration, while 4.9 eV UV exposure decreases the  $P_b$  concentration.<sup>12</sup> With the observation of the depleted  $P_b$  centers during plasma processing, this indicates that photons in the UV



**Figure 4.** (Color online) (a) ESR signals and (b) corresponding defect-state concentrations for  $\text{HfO}_2$  covered samples (photons) and uncovered samples (ions and photons) with the capillary-array window before and after plasma exposure.

range appear to be more likely than photons in the VUV range in modifying the defect-state concentration during plasma exposure. This is also verified by the fact that as the photon energies increases from the UV range to the VUV range, the penetration depth of the photons becomes smaller.<sup>21</sup>

Furthermore, in order to verify the plasma ion and photon bombardment penetration depths, a capillary-array window<sup>22</sup> was used to cover a portion of the dielectric sample. The capillary-array window filters out the ion flux while allowing photons to pass through to the dielectric. Plasma exposure was then made simultaneously on the covered and uncovered dielectric samples and the results were compared.

After simultaneous plasma exposure of the covered and uncovered samples, ESR measurements were made, as shown in Fig. 4. From Fig. 4, it can be seen that photon bombardment reduces the  $P_b$  concentrations in  $\text{HfO}_2$ . From analysis of the uncovered sample, the addition of ion bombardment does not modify the defect concentrations significantly. This verifies that most of the defect-state modifications were due to photon bombardment.

Based on the observation that ions introduce charge accumulation and photons in the UV range dominate in reducing the defect-state concentrations, in order to reduce both charging and defect-state concentrations, a lower ion fluence and a higher photon fluence are needed. From Fig. 1 and the above discussion, the best way to

achieve this condition is to reduce the neutral pressure of the plasma. As microwave power changes, a tradeoff is observed between the charge reduction and the defect depletion. From Fig. 1, the optimal operating conditions are 5 mTorr of pressure and 200 W of microwave power. In this case an ion fluence of  $4.8 \times 10^{14}$  ions/cm<sup>2</sup> and a photon fluence of  $8.4 \times 10^{15}$  photons/cm<sup>2</sup> were obtained for 10-min plasma exposure. Ten minutes of plasma exposure was used so as to create a sufficient fluence in order to maximize the damage to the dielectric samples.

With these plasma conditions, the charge accumulation resulted in a surface potential of 1.9 V and the  $P_{b0}$  and  $P_{b1}$  centers showed concentrations of  $2.8 \times 10^{11}$  and  $1.3 \times 10^{11}$  cm<sup>-2</sup> that are all minimum values. It must be pointed out that because of the differences between the various plasma-processing systems as well as different types of processing, the ideal operating conditions may vary. However, with the methodology proposed in this article, it is not hard to find out the local optimum.

In conclusion, plasma conditions, i.e., pressure and microwave power, are related to the ion and photon fluxes. Ion fluence was shown to contribute mostly to the charge accumulation on the surface of the dielectric films, while photon fluence contributes primarily to modifying the concentration of interfacial defect states. Increasing the photon fluence during plasma exposure was helpful in depleting the interlayer defects. It was found that in order to optimize charge reduction and defect depletion, the plasma operating pressure should be as low as possible, consistent with the processing requirements. This methodology can be applied to various plasma-processing systems to find optimal operation conditions for processing various dielectric materials.

We thank M. Ivancic for helping set up the ESR experiments. This work is supported by the Semiconductor Research Corporation under Contract no. 2008-KJ-1781.

## References

- S. Fang and J. P. McVittie, *IEEE Electron Device Lett.*, **13**, 288 (1992).
- K. P. Cheung and C. S. Pai, *IEEE Electron Device Lett.*, **16**, 220 (1995).
- A. Stesmans and V. V. Afanas'ev, *Appl. Phys. Lett.*, **85**, 3792 (2004).
- B. B. Triplett, P. T. Chen, Y. Nishi, P. H. Kasai, J. J. Chambers, and L. Colombo, *J. Appl. Phys.*, **101**, 013703 (2007).
- A. Grill and V. Patel, *J. Appl. Phys.*, **85**, 3314 (1999).
- H. Moon, S. K. Cho, R. L. Garrell, and C.-J. Kim, *J. Appl. Phys.*, **92**, 4080 (2002).
- K. Yonekura, S. Sakamori, K. Goto, M. Matsuura, N. Fujiwara, and M. Yoneda, *J. Vac. Sci. Technol. B*, **22**, 548 (2004).
- S. Uchida, S. Takashima, M. Hori, M. Fukasawa, K. Ohshima, K. Nagahata, and T. Tatsumi, *J. Appl. Phys.*, **103**, 073303 (2008).
- H. Ren, G. A. Antonelli, Y. Nishi, and J. L. Shohet, *J. Appl. Phys.*, **108**, 094110 (2010).
- K. Y. Fu, X. Tian, and P. K. Chu, *Rev. Sci. Instrum.*, **74**, 3697 (2003).
- D. Nest, T.-Y. Chung, D. B. Graves, S. Engelmann, R. L. Bruce, F. Weirnboeck, G. S. Oehrlein, D. Wang, C. Andes, and E. A. Hudson, *Plasma Processes Polym.*, **6**, 649 (2009).
- H. Ren, S. L. Cheng, Y. Nishi, and J. L. Shohet, *Appl. Phys. Lett.*, **96**, 192902 (2010).
- M. Tabib-Azar, D. Akinwande, G. E. Ponchak, and S. R. LeClair, *Rev. Sci. Instrum.*, **70**, 3083 (1999).
- B. D. Beake, J. S. G. Ling, and G. J. Leggett, *J. Mater. Chem.*, **8**, 1735 (1998).
- M. A. Lieberman and A. J. Lichtenberg, *Principles of Plasma Discharges and Materials Processing*, John Wiley & Sons, New York (1999).
- L. Oksuz and N. Hershkowitz, *Phys. Rev. Lett.*, **89**, 145001 (2002).
- A. Smirnov, Y. Raitsev, and N. J. Fisch, *J. Appl. Phys.*, **94**, 852 (2003).
- K. U. Riemann, *J. Phys. D: Appl. Phys.*, **24**, 493 (1991).
- N. Hershkowitz, in *Plasma Diagnostics*, O. Auciello and D. L. Flamm, Editors, Academic, New York (1993).
- E. H. Poindexter, P. J. Caplan, B. E. Deal, and R. R. Razouk, *J. Appl. Phys.*, **52**, 879 (1981).
- G. A. Shaw, A. M. Siegel, J. Model, A. Geboff, S. Soloviev, A. Vert, and P. Sandvik, *Proc. SPIE*, **7320**, 73200J (2009).
- J. D. Chatterton, G. S. Upadhyaya, J. L. Shohet, J. L. Lauer, R. D. Bathke, and K. Kukkady, *J. Appl. Phys.*, **100**, 043306 (2006).